JACS
JOURNAL OF THE AMERICAN CHEMICAL SOCIETY

ARTICLE

pubs.acs.org/JACS

Mechanism of Cobalt(II) Porphyrin-Catalyzed C−H Amination with Organic Azides: Radical Nature and H-Atom Abstraction Ability of the Key Cobalt(III)−Nitrene Intermediates

Volodymyr Lyaskovskyy,[†] Alma I. Olivos Suarez,[†] Hongjian Lu,[‡] Huiling Jiang,[‡] X. Peter Zhang,*[,‡] and Bas de Bruin*[,†]

[†]Van 't Hoff Institute for Molecular Sciences (HIMS), Homogeneous and Supramolecular Catalysis, University of Amsterdam, Science Park 904, 1098 XH Amsterdam, The Netherlands

[‡]Department of Chemistry, University of South Florida, Tampa, Florida 33620-5250, United States

Supporting Information

ABSTRACT: The mechanism of cobalt(II) porphyrin-catalyzed benzylic C−H bond amination of ethylbenzene, toluene, and 1,2,3,4-tetrahydronaphthalene (tetralin) using a series of different organic azides [$N_3C(O)OMe$, N_3SO_2Ph, $N_3C(O)Ph$, and $N_3P(O)(OMe)_2$] as nitrene sources was studied by means of density functional theory (DFT) calculations and electron paramagnetic resonance (EPR) spectroscopy. The DFT computational study revealed a stepwise radical process involving coordination of the azide to the metal center followed by elimination of dinitrogen to produce unusual "nitrene radical" intermediates (por)Co^{III}−$N^{\bullet}Y$ (**4**) [Y = −C(O)OMe, $-SO_2Ph$, −C(O)Ph, $-P(O)(OMe)_2$]. Formation of these nitrene radical ligand complexes is exothermic, predicting that the nitrene radical ligand complexes should be detectable species in the absence of other reacting substrates. In good agreement with the DFT calculations, isotropic solution EPR signals with *g* values characteristic of ligand-based radicals were detected experimentally from (por)Co complexes in the presence of excess organic azide in benzene. They are best described as nitrene radical anion ligand complexes (por)Co^{III}−$N^{\bullet}Y$, which have their unpaired spin density located almost entirely on the nitrogen atom of the nitrene moiety. These key cobalt(III)−nitrene radical intermediates readily abstract a hydrogen atom from a benzylic position of the organic substrate to form the intermediate species **5**, which are close-contact pairs of the thus-formed organic radicals $R'^{\bullet}$ and the cobalt(III)−amido complexes (por)Co^{III}−*NHY* ({$R'^{\bullet}\cdots$(por)Co^{III}−*NHY*}). These close-contact pairs readily collapse in a virtually barrierless fashion (via transition state **TS3**) to produce the cobalt(II)−amine complexes (por)Co^{II}−*NHY*R′, which dissociate to afford the desired amine products *NHY*R′ (**6**) with regeneration of the (por)Co catalyst. Alternatively, the close-contact pairs {$R'^{\bullet}\cdots$(por)Co^{III}−*NHY*} **5** may undergo *β*-hydrogen-atom abstraction from the benzylic radical $R'^{\bullet}$ by (por)Co^{III}−*NHY* (via **TS4**) to form the corresponding olefin and (por)Co^{III}−NH_2Y, which dissociates to give Y−NH_2. This process for the formation of olefin and Y−NH_2 byproducts is also essentially barrierless and should compete with the collapse of **5** via **TS3** to form the desired amine product. Alternative processes leading to the formation of side products and the influence of different porphyrin ligands with varying electronic properties on the catalytic activity of the cobalt(II) complexes have also been investigated.

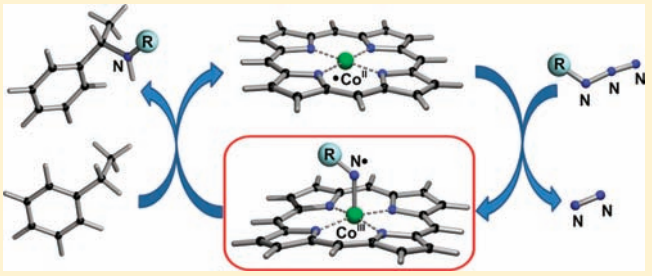

INTRODUCTION

Direct functionalization of C−H bonds is of outstanding importance because of its far-reaching practical applications as atom-, time-, and cost-efficient alternatives to traditional hydrocarbon functionalization approaches, which involve stepwise stoichiometric modifications.[1] This has led to the development of prominent methodologies for hydrocarbon transformations such as palladium-catalyzed cross-coupling of C−H bonds[2] and C−H insertion of carbenoid and nitrenoid species[3] as well as a number of efficient protocols for selective modification of nonactivated alkanes.[4] Numerous applications of amines have stimulated an intensive exploration of direct C−H amination methods.[3,5] These reactions typically employ iminoiodanes (i.e., PhI═NTs),[6] haloamine-T compounds,[6a,7] carbamates,[6a,8] or azides[6a,9] as the nitrene sources. Among several catalysts that have been tested, the most successful ones are probably still those based on expensive Rh[3,10] and Ru[3,11] complexes, although less costly Mn-,[12] Cu-,[7b−d,8c,9i] and Fe-based[13] catalysts have also been reported. Organic azides are among the most promising and environmentally friendly nitrene sources for these reactions, for which a large substrate scope is available. Similar to carbene formation from diazo reagents, azides can generate nitrene ligands at transition metals by a simple loss of harmless

Received: May 25, 2011
Published: June 28, 2011

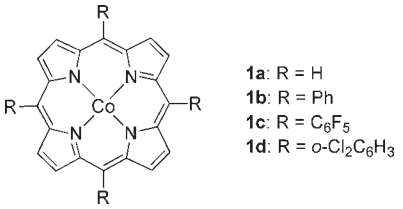

Figure 1. Structures of cobalt(II) porphyrin catalysts: R = H, Co(por) (**1a**); R = Ph, Co(TPP) (**1b**); R = C_6F_5, Co(TPFPP) (**1c**); R = o-$Cl_2C_6H_3$, Co(TDClPP) (**1d**).

dinitrogen as the only byproduct. While most of the known catalysts are quite effective with iminoiodanes, currently only a limited number of catalysts for C−H amination are capable of employing organic azides, which are much more desirable nitrene sources.

Cobalt(II) porphyrin catalysts **1** (Figure 1) have attracted considerable attention as a result of their unique reactivity in carbene-transfer reactions.[14] They are also efficient catalysts for olefin aziridination employing an organic azide as the nitrene source.[15] Quite recently, in line with the topic of this paper, they have also been reported to be efficient catalysts for amination of benzylic C−H bonds with organic azides (Scheme 1).[9d] This reaction proved to be quite sensitive to the structure and nature of the employed organic azide, C−H substrate, and catalyst. Whereas 2,2,2-trichloroethoxycarbonyl azide [$CCl_3CH_2OC(O)N_3$; $TrocN_3$] was found to be an excellent nitrene source (or amination reagent) for producing target amines in high yields, tosyl azide (TsN_3) demonstrated only modest reactivity, and benzoyl azide (BzN_3) and dimethyl azidophosphate [$(MeO)_2P(O)N_3$] showed no reactivity.[9d] In addition, the activity of the cobalt(II)-based catalysts was rather unexpected. For example, the catalysts Co(TPFPP) (**1c**) and Co(TDClPP) (**1d**), which had previously proven to be efficient in C−H amination reactions employing bromamine-T as the nitrene source,[7a] were inactive with organic azides. On the other hand, Co(TPP) (**1b**), which showed only rather poor catalytic reactivity with bromamine-T, turned out to be a quite effective catalyst for aminations employing organic azides.

Cenini and co-workers reported a kinetic study of the Co(por)-catalyzed C−H amination reaction of benzylic derivatives with aryl azides.[9f,g] The reaction was found to exhibit overall third-order reaction kinetics (first-order with respect to the catalyst, the azide, and the benzylic substrate).

A detailed mechanistic investigation is indispensable to gain a better understanding of the cobalt(II)-catalyzed C−H amination reactions and should assist in addressing further selectivity issues. Such insights are also important to aid future investigations to expand the substrate scope and for the design of new efficient catalysts. Insight into the key active species of these reactions is of crucial importance for understanding the influence of the different steric and electronic factors on the rate and outcome of these processes. To the best of our knowledge, transition-metal-catalyzed amination of benzylic C−H bonds by organic azides has not previously been studied either theoretically or by EPR spectroscopy, in contrast to amination of alkenyl and aryl C−H bonds, which react via a different pathway.[11c] Amination of allylic C−H bonds with phenyl azide (PhN_3), which gives rather poor yields and poor selectivity in experimental nitrene transfer/insertion reactions, was recently examined in the context of Co(por)-catalyzed aziridination reactions.[16] Herein we present

Scheme 1. Catalytic C−H Amination of Benzylic C−H Bonds with Azides

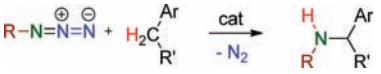

an EPR spectroscopic and detailed computational study of the mechanism of the Co(por)-catalyzed amination of benzylic C−H bonds by a series of different organic azides. The computational investigations include an examination of how varying the electronic properties of the porphyrin ligand of the Co(por) catalyst affects the rate-limiting steps (via transition states **TS1** and **TS2**) of the catalytic reactions. Remarkably, the mechanism we propose here appears to be a rather general process, since an analogous pathway has also been suggested for non-heme iron-catalyzed aliphatic C−H hydroxylation and amination reactions.[17] The latter, however, has not been studied computationally to date.

RESULTS AND DISCUSSION

Below we will first discuss the detailed catalytic C−H amination mechanism based on our DFT computational studies and validate the obtained results by comparison to the experimental information available to date. On the basis of these DFT results, we will then focus on our experimental detection of the proposed key nitrene radical intermediates using EPR spectroscopy. The obtained EPR data are reported as the final account of this paper.

Computational Studies. Calculations were performed by employing the nonhybrid BP86 level of theory, which has been shown to give reliable and satisfactory results for related systems.[14c,18] As a simplified model of the Troc group, we used the methyl formate substituent [MeOC(O)−]. The benzylic C−H substrates were modeled with ethylbenzene, which can also be used as a representative model for 1,2,3,4-tetrahydronaphthalene (tetralin), since the calculated barriers of the rate-limiting steps appeared to be very similar for these two substrates (see below). Experimentally, yields for C−H amination of ethylbenzene and tetralin were reported to be comparable.[9d] We initially used the nonsubstituted complex Co(por) (**1a**, Figure 1) as a smaller model for Co(TPP) (**1b**), which has been reported to be an efficient catalyst for the amination of benzylic C−H bonds.[9d] We further expanded our study to include electronically different porphyrin ligands with varied meso substituents for a selection of the key steps of the mechanism (see below).

We will first discuss the amination of ethylbenzene with methyl azidoformate, a model of $TrocN_3$, which was experimentally shown to be an effective nitrene source for C−H amination. We will then present the computational pathways with phenylsulfonyl azide, benzoyl azide, and dimethyl azidophosphate, which were found experimentally to be less effective nitrene sources. Finally, we will present the influence of different porphyrin ligands on the catalytic activity of Co(por)-based systems in the C−H amination reaction.

Reaction of Ethylbenzene with Methyl Azidoformate. The activation step of methyl azidoformate (**2a**) by Co complex **1a** involves coordination of the α-nitrogen of **2a** to the cobalt(II) center (Scheme 2). This process is exothermic by about −1.8 kcal mol^{-1} (Figure 2). The formed azide complex **3a** undergoes dinitrogen elimination, which leads to formation of the "nitrene" complex **4a**. The activation enthalpy $\Delta H^{\ddagger}$(**TS1a**) for this step is

Scheme 2. Catalytic Cycle for Co(por)-Based C−H Amination with Azide

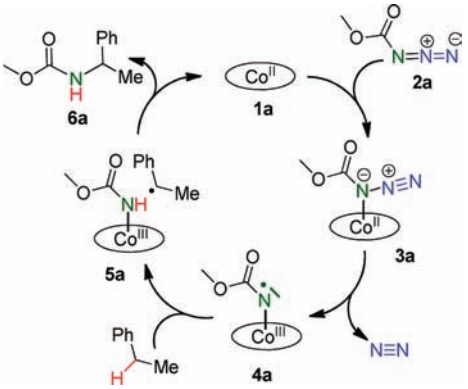

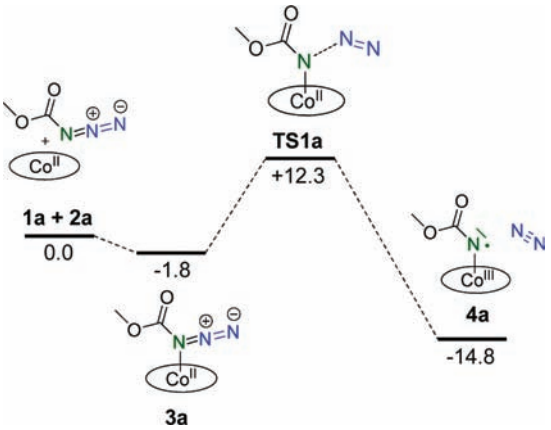

Figure 2. Reaction profile (ΔH in kcal mol^{-1}) for nitrene radical formation from Co(por) and azide **2a**.

+12.3 kcal mol^{-1} (Figure 2), which agrees well with the reaction conditions (40−80 °C) applied experimentally.

The electronic structure of **4a** is noteworthy. It was found that the "nitrene" complex is actually a species with a "nitrene radical ligand", very similar to the "nitrene radical species" that were recently reported to be the key intermediates in olefin aziridination reactions.[16,18a] This feature underlines the general importance of redox non-innocent ligands in catalysis.[19] As illustrated in Figure 3, the unpaired electron resides mainly on the "nitrene" nitrogen [i.e., the nitrogen of the N−C(O)OMe moiety] and is slightly delocalized over the neighboring cobalt and carbonyl oxygen atoms. Accordingly, the "nitrene ligand" is best described as a nitrogen-centered radical ligand $\{RN^{\bullet}\}^{-}$ ("nitrene radical anion ligand").

This gives rise to clear radical-type reactivity at its nitrogen atom, resulting in effective hydrogen-atom abstraction from the benzylic position of ethylbenzene (**TS2a**, Figure 4). This leads to a close-contact catalyst−radical pair (**5a**) of the thus-formed benzylic radical PhC$^{\bullet}$HCH$_3$ (R′$^{\bullet}$) and the cobalt(III)−amido complex (por)Co^{III}−N*H*C(O)OMe. Intermediate **5a** provides a decent but simplified model of the solvent-caged catalyst−radical pair $\{R'^{\bullet}\cdots(por)Co^{III}-NHC(O)OMe\}$, which is expected to play a crucial role in solution (Figure 4). Although the computed activation enthalpy for **TS2a** ($\Delta H^{\ddagger}$ = +6.3 kcal mol^{-1}) is lower than the activation energy for formation of nitrene radical **4a** (**TS1a** = +12.3 kcal mol^{-1}), the two reactions have

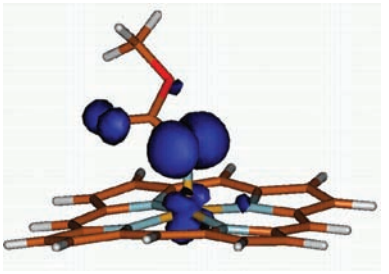

Figure 3. Spin density plot of the DFT-optimized "nitrene radical" species **4a**.[20]

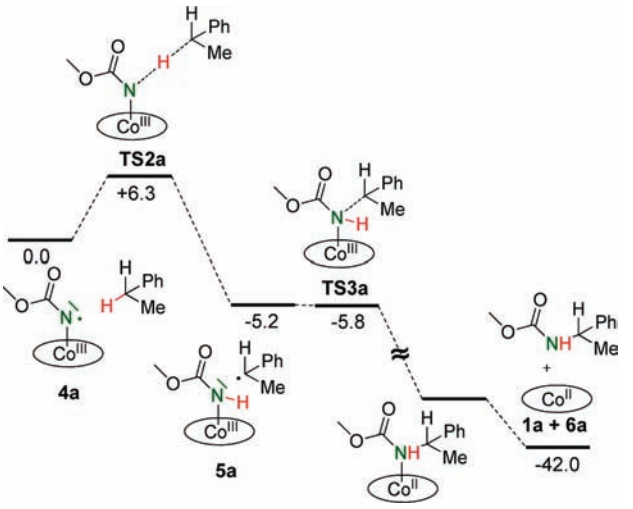

Figure 4. Reaction profile (ΔH in kcal mol^{-1}) for the nitrene insertion reaction into the benzylic C−H bond of ethylbenzene.

quite comparable $\Delta G^{\ddagger}$ values [$\Delta G^{\ddagger}$(**TS1a**) = +20.6 kcal mol^{-1}; $\Delta G^{\ddagger}$(**TS2a**) = +17.0 kcal mol^{-1}]. The energetic data therefore correspond well with the observed first-order kinetics with respect to the catalyst, the azide, and the benzylic/allylic substrate found by Cenini and co-workers for related systems in the C−H amination of cyclohexene, α-methylstyrene, and toluene using *p*-NO_2−$C_6H_4N_3$ as the nitrene source,[9f,g] wherein formation of the nitrene and its subsequent C−H bond activation reactivity should both be rate-limiting processes.[21] The experimental kinetic profile for the exact reactions based on the $TrocN_3$ nitrene source has not been determined to date.

Replacing ethylbenzene with tetralin as the benzylic C−H substrate in the calculations resulted in a marginally lower, almost similar **TS2** barrier [$\Delta H^{\ddagger}$(**TS2**) = +6.2 kcal mol^{-1}; $\Delta G^{\ddagger}$(**TS2**) = +16.7 kcal mol^{-1}]. As expected, the **TS2** barrier for activation of toluene [$\Delta H^{\ddagger}$(**TS2**) = +7.4 kcal mol^{-1}; $\Delta G^{\ddagger}$(**TS2**) = +18.2 kcal mol^{-1}] is higher than for ethylbenzene and tetralin. This correlates with the experimental observation that amination of tetralin is possible even with toluene as the solvent.[9d] The energies of the intermediates and the **TS3** barrier for the following steps with toluene are very similar to those with ethylbenzene and do not constitute any additional rate-limiting barriers (see the Supporting Information).

The catalyst−radical pair $\{R'^{\bullet}\cdots(por)Co^{III}-NHC(O)OMe\}$ **5a**[22] undergoes very facile radical substitution (a rebound-type reaction), in which the "free" benzylic radical back-attacks the nitrogen atom of the (por)Co^{III}−N*H*C(O)OMe species to form the target amide product **6a** (Figure 4). This step is essentially

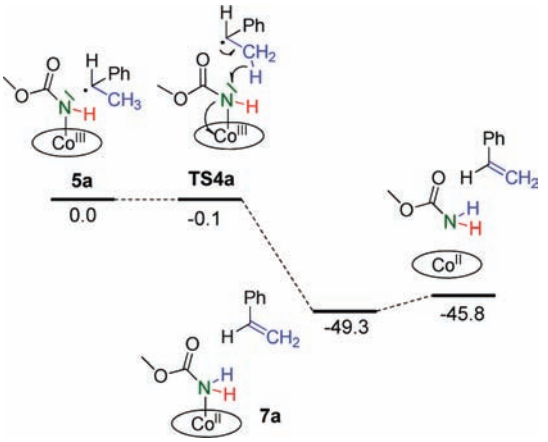

Figure 5. Reaction profile (ΔH in kcal mol^{-1}) for formation of olefin byproducts.

barrierless on the enthalpy surface (a small-barrier transition state, **TS3a**, was located on the SCF surface; ΔE = +0.1 kcal mol^{-1}). Carbamate **6a** was found to be very weakly coordinated to the Co center, and its dissociation occurred during the geometry optimization steps.

Formation of Byproducts. Experimentally, $TrocNH_2$ is formed as a main byproduct under the applied reaction conditions.[9d] Initially, we assumed that this byproduct would be formed as a result of homolysis of the Co−N bond in intermediate **5a**.[9d] However, this seems rather unlikely on the basis of the DFT calculations. Although the Co−N bond dissociation enthalpy (BDE) of +39.4 kcal mol^{-1} is perhaps not particularly high as an absolute value,[23] it is much higher than the **TS1** and **TS2** barriers. Therefore, the barriers for side reactions proceeding via direct homolytic bond splitting of the Co−N bond of **5a** should be at least equal to or perhaps even higher than this BDE value, and thus, these side reactions should compete poorly. However, hydrogen-atom transfer from a C−H bond at the β-position of the "free" benzylic radical to the amido nitrogen atom in the {R′$^{\bullet}\cdots$(por)Co^{III}−N*H*C(O)OMe} catalyst−radical pair **5a** (a reaction bearing some similarity with radical disproportionation by free radicals bearing β-hydrogens) is well-supported by the DFT calculations (Figure 5). As for the radical-rebound step in Figure 4, this reaction is essentially barrierless on the enthalpy surface (a small-barrier transition state, **TS4a**, was located on the SCF surface; ΔE = +1.8 kcal mol^{-1}). The productive rebound steps in Figure 4 and the steps leading to byproducts in Figure 5 should thus compete, in good agreement with the experiments. Even though the processes leading to the target insertion product (**TS3a**) and to the byproduct (**TS4a**) have similar activation enthalpies, the former is favored on the free energy surface [$\Delta G^{\ddagger}$(**TS3a**) = +1.2 kcal mol^{-1} vs $\Delta G^{\ddagger}$(**TS4a**) = +3.8 kcal mol^{-1}]. This explains the fact that the insertion product is experimentally the major compound in most cases.[9d]

The formation of $TrocNH_2$ via β-hydrogen abstraction from the benzylic organic radical should lead to the formation of an alkene co-byproduct. Indeed, experimental reinvestigation of the catalytic C−H amination of ethylbenzene with GC−MS revealed the formation of styrene as a byproduct.

It is noted that a large amount of $TrocNH_2$ was also observed in the amination reaction of ethyl phenylacetate [$PhCH_2C(O)OEt$], which has no C−H bonds at the β-position of its reactive benzylic moiety.[9d] This indicates the existence of another pathway for

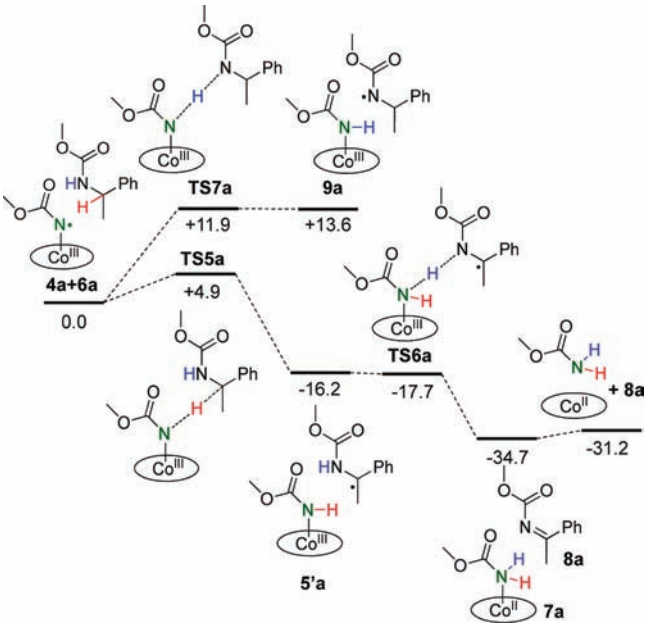

Figure 6. Reaction profile (ΔH in kcal mol^{-1}) for the alternative pathway for $TrocNH_2$ byproduct formation involving hydrogen abstraction from amide **6a** by nitrene complex **4a**.

formation of the $TrocNH_2$ byproduct, because the pathway depicted in Figure 5 requires the presence of β-hydrogen atoms. In this case, we assumed that the formation of the byproduct is due to a subsequent hydrogen-atom abstraction from the amine product. We modeled this possibility using **6a** as the substrate. Hydrogen-atom abstraction from the benzylic position of **6a** by the nitrene radical complex **4a** followed by hydrogen-atom transfer from the intermediate radical to the Co−NHCOOMe intermediate **5′a** would lead to imine **8a** (Figure 6). The latter most likely decomposes to $MeOC(O)NH_2$ and a corresponding carbonyl compound during purification by column chromatography on silica under the applied experimental conditions. The abstraction of the hydrogen atom from the benzylic position of amine **6a** proceeds with a small barrier (**TS5a** = +4.9 kcal mol^{-1}) and leads to intermediate **5′a**, which is a close catalyst−radical pair {R′$^{\bullet}\cdots$(por)Co^{III}−N*H*C(O)OMe} wherein R′$^{\bullet}$ is the corresponding benzyl radical MeOC(O)NHC$^{\bullet}$(Ph)Me (Figure 6). This step is also thermodynamically favorable, with ΔH° = −16.2 kcal mol^{-1}. Since the alternative abstraction of a hydrogen atom from the NH group has a rather high barrier of 11.9 kcal mol^{-1}, it is considered to be much less probable[24] (Figure 6; for the whole reaction profile of the NH hydrogen abstraction, see the Supporting Information). Moreover, intermediate **9a** was found to be rather unstable and should undergo a rapid reverse interconversion into the starting species **4a** and **6a**.

In the formed intermediate **5′a**, hydrogen-atom transfer from the amine NH moiety at the β-hydrogen position of the benzylic radical to the cobalt−amido nitrogen atom then leads to the formation of the $MeOC(O)NH_2$ byproduct and imine **8a**. This process is again essentially barrierless (a small-barrier transition state, **TS6a**, was located on the SCF surface; ΔE = +0.7 kcal mol^{-1}).

As shown in Figure 6, the formation of the $TrocNH_2$ byproduct by hydrogen abstraction from the final amide **6a** has a higher kinetic barrier and is energetically less favorable than the β-hydrogen-atom transfer pathway in Figure 5. Therefore, the

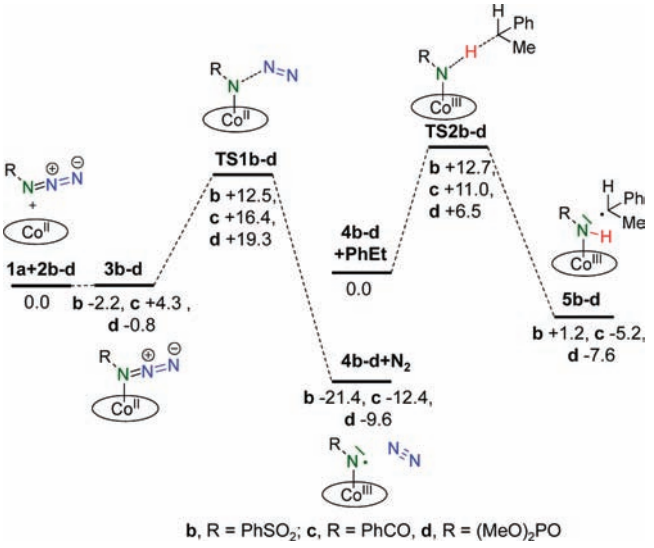

Figure 7. Reaction profile (ΔH in kcal mol^{-1}) for C−H bond amination employing phenylsulfonyl azide (**2b**), benzoyl azide (**2c**), or dimethyl azidophosphate (**2d**) as the nitrene source.

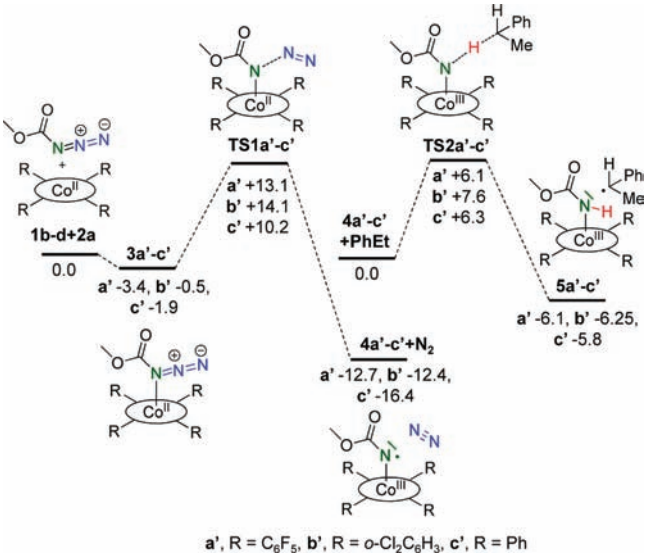

Figure 8. Reaction profile (ΔH in kcal mol^{-1}) for C−H amination employing catalysts **1b**−**d** (see Figure 1 for the structures of the catalysts).

pathway in Figure 5 should prevail for substrates containing hydrogen atoms at the β-position with respect to the benzylic radical. However, the alternative mechanism in Figure 6 is a viable pathway for $TrocNH_2$ byproduct formation in reactions featuring substrates lacking such β-hydrogen atoms.

Influence of Different Organic Azides. The successful experimental use of $TrocN_3$ as a nitrene source raises the question of why the other tested azides showed either rather poor reactivity (e.g., TsN_3 gave only 32% yield of the target amide) or no reactivity at all [e.g., $(EtO)_2P(O)N_3$ and $PhCON_3$].[9d] To shed some light on this issue, we carried out quantum-chemical calculations of the two rate-limiting steps (**TS1** and **TS2**) for phenylsulfonyl azide (**2b**), benzoyl azide (**2c**), and dimethyl azidophosphate (**2d**) (Figure 7).

While coordination of the azide to Co(por) proceeds as a slightly exothermic reaction for **2b** ($\Delta H°$ = −2.2 kcal mol^{-1}) and **2d** ($\Delta H°$ = −0.8 kcal mol^{-1}), it is endothermic for **2c** ($\Delta H°$ = +4.3 kcal mol^{-1}) (Figure 7).

The elimination of dinitrogen to form the nitrene radical species **4b**−**d** (Figure 7) is in all cases associated with a higher barrier than the analogous reaction with methyl azidoformate **2a** [$\Delta H^{‡}$(**TS1a**) = +12.3 kcal mol^{-1}; see Figure 2]. The spin density at the nitrogen atom in species **4a**−**d** depends slightly on the nature of the R group, resulting in somewhat more localized radical density at the "nitrene" nitrogen nucleus for species **2a** and **2d**.[20]

Whereas the energy barrier ($\Delta H^{‡}$) of the first step (**TS1**) is only slightly higher in the case of phenylsulfonyl azide [$\Delta H^{‡}$(**TS1b**) = +12.5 kcal mol^{-1}], it is substantially higher for benzoyl azide [$\Delta H^{‡}$(**TS1c**) = +16.4 kcal mol^{-1}] and azidophosphate [$\Delta H^{‡}$(**TS1d**) = +19.3 kcal mol^{-1}]. Thermodynamically, however, all of the reactions are exothermic, with $\Delta H°$ = −21.4, −12.4, and −9.6 kcal mol^{-1} for the formation of phenylsulfonyl derivative **4b**, benzoyl nitrene **4c**, and azidophosphate species **4d**, respectively. Interestingly, the **TS1** energy barrier seems to be correlated with the Nα−Nβ bond length in the azide [Nα−Nβ bond lengths = 1.243 Å (**2a**), 1.239 Å (**2b**), 1.240 Å (**2c**), and 1.236 Å (**2d**)]. Only arylsulfonyl derivative **2b** is slightly out of this general trend. A longer Nα−Nβ bond distance typically indicates a lower bond energy, which in turn should lead to a lower **TS1** barrier.

The activation energy of the second step also differs quite substantially for the studied azides (Figure 7). Thus, the phenylsulfonyl and benzoyl derivatives have relatively high $\Delta H^{‡}$(**TS2**) barriers of +12.7 and +11.0 kcal mol^{-1}, respectively, whereas the dimethoxyphosphoryl nitrene shows a moderate barrier of +6.5 kcal mol^{-1}. While the formation of the benzylic radical is exothermic by −5.2 and −7.6 kcal mol^{-1} for the benzoyl and phosphoryl derivatives, respectively, it is slightly endothermic by +1.2 kcal mol^{-1} for the phenylsulfonyl derivative. For the phenylsulfonyl derivative, the combination of a higher **TS1** barrier and the substantially increased **TS2** barrier should make the nitrene insertion reaction quite slow, leading to moderate yields. For the benzoyl and phosphate azides, the **TS2** barriers (second step: H-atom abstraction) are quite low, but the **TS1** barriers for nitrene radical formation (first step: dinitrogen elimination) are much higher, which explains the poor reactivity of these substrates in the C−H insertion reactions. This fact may be attributed to a comparatively high Nα−Nβ bond energy in the two latter azides. These data are in excellent agreement with the experimental observations.[9d]

Co(por) Catalysts with Different Substituents. Intrigued by the variation in the activities of different catalysts, we also carried out a computational study of the two rate-limiting steps (**TS1** and **TS2**) for catalysts **1c** and **1d** (Figures 1 and 8). As clearly shown in Figure 8, substitution of the meso hydrogens of the porphyrin ring by electron-withdrawing perfluorophenyl and 2,6-dichlorophenyl groups leads to an increase in the **TS1** activation barrier for nitrene radical formation from +12.3 kcal mol^{-1} for the unsubstituted Co(por) complex **1a** to +13.1 and +14.1 kcal mol^{-1} for **1c** and **1d**, respectively (Figures 1 and 8). This effect is even more evident for the comparative DFT calculations using the experimentally most successful Co(TPP) catalyst **1b**, which has a remarkably low $\Delta H^{‡}$(**TS1c′**) of only +10.2 kcal mol^{-1} (Figure 8). Thermodynamically, all of the reactions are exothermic processes, with $\Delta H°$ values

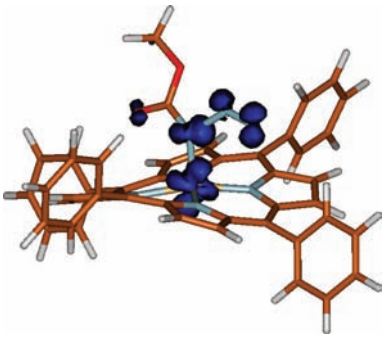

Figure 9. Spin density plot of the DFT-optimized transition state **TS1c′** leading to formation of the "nitrene radical" species.

of −12.7, −12.4, and −16.4 kcal mol^{-1} for the formation of **4a′**, **4b′**, and **4c′**, respectively.

The energies of the second hydrogen-atom abstraction steps (**TS2**) are comparable for all of the catalysts (Figures 4 and 8), with $\Delta H^{\ddagger}$(**TS2**) barriers of +6.3 kcal mol^{-1} for the Co(TPP) and Co(por) catalysts and +6.1 and +7.6 kcal mol^{-1} for the perfluorophenyl- and 2,6-dichlorophenyl-substituted porphyrin complexes **4a′** and **4b′**, respectively. Hence, the electronic influence of the meso substituents has a much bigger influence on the first step (**TS1**) of the catalytic reaction.

For efficient formation of the nitrene intermediates **4**, it seems apparent that a catalyst should bear groups with rather mild electron-withdrawing properties at the meso positions of the porphyrin ring. Groups that are too strongly electron-withdrawing (e.g., C_6F_5− and 2,6-$Cl_2C_6H_3$−) would be ineffective, whereas having no substituent at the meso position at all (as in catalyst **1a**) would also lead to a decrease in catalytic activity. On one hand, electron-withdrawing groups are beneficial for the reaction because they enhance the formation of the Co−N bond in the azide adducts **3** and thereby weaken the Nα−Nβ bond of the azide, but on the other hand, elimination of nitrogen in the transition states **TS1** involves considerable oxidation of the metal center by electron transfer to the nitrene nitrogen. For example, in the transition states **TS1a′**−**c′**, ∼20% of the unpaired electron has already been transferred to the "nitrene" nitrogen (Figure 9).[25] Since having groups that are too strongly electron-withdrawing at the meso positions of the porphyrin in the catalyst raise the redox potential of cobalt in the corresponding complexes, this hampers the internal electron transfer from cobalt to nitrogen, resulting in higher activation energies for nitrogen elimination. Therefore, the optimal Co(por) catalysts for this reaction must have subtly balanced electronic properties.

Implications for (Optimizing) the Catalytic Reactions. The above computational study has provided rather detailed answers to central mechanistic questions concerning (por)Co-catalyzed C−H bond amination reactions using an organic azide as the nitrene source. These insights hint at a window of opportunities in exploring the substrate scope and seeking the optimal reaction conditions and the best catalysts. These catalytic implications are briefly summarized in this section.

Elimination of dinitrogen from the azide adduct to form the "nitrene radical" intermediate (**TS1**) and subsequent benzylic hydrogen abstraction by this intermediate (**TS2**) are both kinetically important. The effectiveness of an azide as nitrene source is mainly determined by the activation energies of these two steps. The poor reactivity of the benzoyl and dimethoxyphosphoryl azides can be attributed to the high **TS1** activation barriers for dinitrogen elimination. In case of phenylsulfonyl azide, a rather high barrier for the hydrogen abstraction step (**TS2**) is likely responsible for its low reactivity. The lowest combined **TS1** and **TS2** barriers for the $N_3C(O)OMe$-based amination are in good agreement with the fact that $N_3C(O)OCH_2CCl_3$ ($TrocN_3$) is the optimal nitrene source in this series.[9d] Differences in the **TS2** barriers further largely determine the substrate, regio-, and product selectivities.

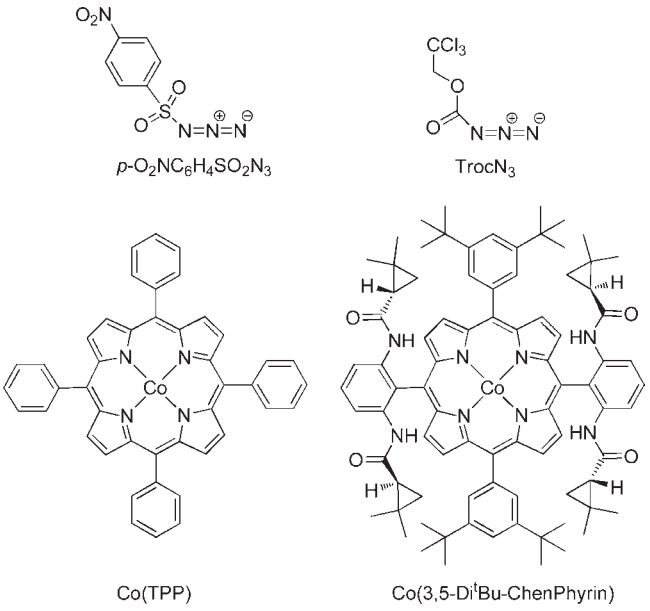

Figure 10. Organic azides and cobalt(II) porphyrin complexes used in the EPR studies.

The initial dinitrogen elimination (**TS1**) can be considered as the most challenging step of the entire catalytic process. Changes in the structure of the azide as well as the catalyst have a large influence on the activation energy of this step. Electron-withdrawing groups at the meso positions of the porphyrin ligand of the catalyst enhance the formation of the Co−N bond in the azide adduct and thus lower the barrier for N_2 loss. However, since elimination of dinitrogen gas from the azide adduct effectively involves partial electron transfer from the metal to the "nitrene" nitrogen, the use of groups that are too strongly electron-withdrawing at the porphyrin meso positions of the catalyst has a detrimental effect because it raises the redox potential of cobalt in the corresponding complexes. Cobalt complexes of porphyrins with rather mild electron-withdrawing properties thus appear to be the most effective catalysts. Further catalyst improvements should mainly be focused on the facilitation of this step, in which the non-redox-innocence of the nitrene moiety plays a crucial role. Metal complexes that enable effective dinitrogen elimination from the azide to generate a nitrogen-centered radical are essential. Complexes appended with H-bond donors [e.g., Co(3,5-Di^{t}Bu-ChenPhyrin; see Figure 10] are particularly interesting in this respect and should lower the **TS1** barriers significantly, as they do in case of related aziridination reactions.[18] We expect much from catalytic amination reactions with such complexes in the near future.

EPR Spectroscopy. The above DFT studies, as well as our previous computational investigations,[18a] revealed that the formation of nitrene radical complexes of the type (por)Co(N$^{\bullet}$R)

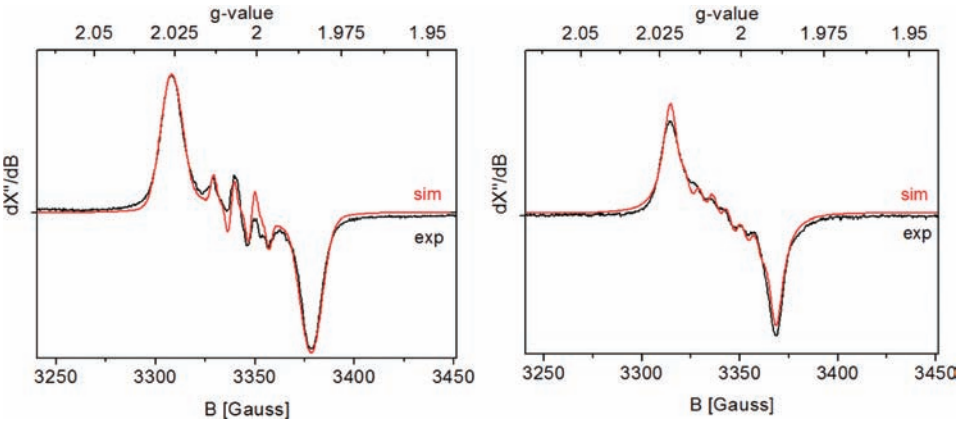

Figure 11. (left) Experimental and simulated isotropic EPR spectra (benzene solution) of (TPP)Co($N^{\bullet}SO_2C_6H_4p$-NO_2) at room temperature (frequency = 9.38056 GHz; modulation amplitude = 1 G; microwave power = 0.2 mW).[26] (right) Experimental and simulated isotropic EPR spectra (benzene solution) of (3,5-Di^{t}Bu-ChenPhyrin)Co($N^{\bullet}$Troc) measured at room temperature (frequency = 9.3791 GHz; modulation amplitude = 0.5 G; microwave power = 0.2 mW).

Table 1. Experimental[a] and DFT-Calculated[b] EPR Parameters[26]

		A_{iso} (MHz)[c]		ρ (%)[d]	
compound	g_{iso}	Co	N	Co	N
(TPP)Co($N^{\bullet}SO_2C_6H_4p$-NO_2)[a]	2.004	24.7	10.0		
I[b]	2.008	20.0	14.8	4	82
(3,5-Di^{t}Bu-ChenPhyrin)Co($N^{\bullet}$Troc)[a]	2.005	19.0	6.0		
II[b]	2.000	26.8	22.1	0.3	90

[a] Parameters from spectral simulations. [b] ORCA, B3LYP/def2-TZVP. [c] Hyperfine couplings. [d] Mulliken spin densities (ORCA, B3LYP/def2-TZVP).

upon reaction of (por)Co species with organic azides is exothermic. Hence, in the absence of other reacting substrates, these species should be detectable. Quite remarkably, however, they have never been detected before, despite their interesting electronic structure. Therefore, we decided to study the reactions of the porphyrin complexes Co(TPP) and Co(3,5-Di^{t}Bu-ChenPhyrin) with the organic azides p-$O_2NC_6H_4SO_2N_3$ and $TrocN_3$ using solution EPR spectroscopy (Figure 10). As discussed above, Co(TPP) is an active catalyst for nitrene insertion reactions of C−H bonds, while Co(por) complexes appended with amido H-bond donors, such as Co(3,5-Di^{t}Bu-ChenPhyrin), are the most active catalysts for olefin aziridination reactions.[15] These reactions proceed via mechanisms involving similar nitrene radical ligand complexes as the key intermediates in the catalytic cycle.[18a]

Excess p-$NO_2C_6H_4SO_2N_3$ and $TrocN_3$ were added to solutions of Co(TPP) and Co(3,5-Di^{t}Bu-ChenPhyrin), respectively, in benzene-d_6, and the solutions were shaken for 10−30 min at room temperature under an inert nitrogen atmosphere. Isotropic solution EPR spectra were recorded on a standard X-band EPR spectrometer. Clear, well-resolved EPR signals were detected that are characteristic of the nitrene radical ligand complexes (Figure 11). While the isotropic g values are clearly characteristic of an $S = {}^1/_2$ organic-ligand-based radical, the signals do show well-resolved hyperfine coupling patterns with cobalt ($I = {}^7/_2$). Hyperfine couplings with a single nitrogen nucleus were apparent from line shape analysis by spectral simulations. Satisfactory simulations were obtained,[26] yielding the cobalt and nitrogen hyperfine couplings listed in Table 1.

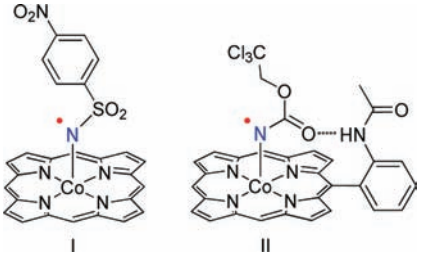

Figure 12. Model compounds used for EPR property calculations.

The EPR parameters of (TPP)Co($N^{\bullet}SO_2C_6H_4p$-NO_2) and (3,5-Di^{t}Bu-ChenPhyrin)Co($N^{\bullet}$Troc) were also calculated using DFT based on the simplified models **I** and **II** shown in Figure 12. The computed EPR data are in qualitative agreement with the experimental data (Table 1). Table 1 also includes the computed spin density distribution at the B3LYP/def2-TZVP level of theory. The nitrogen hyperfine couplings derived from the spectral simulations are smaller than those calculated using DFT (especially for **II**), but considering the use of these simplified gas-phase models, the agreement is quite decent.[27]

The obtained EPR results are quite surprising in view of the fact that the Co(por)-based nitrogen-centered radical ligands were never detected before, although they have frequently been proposed as key intermediates in nitrene transfer chemistry with Co(por) catalysts. We take these EPR data as the first direct experimental evidence for the formation of cobalt(III)−nitrene radical complexes upon reaction of Co(por) species with organic azides. The spin density of these species is clearly centered on the nitrene ligand (also see Figure 3), which is of crucial importance for understanding the reactivity of the key nitrene intermediates in the above-described C−H amination reactions as well as those in related olefin aziridination reactions.[18a] Our current efforts are focused on the detailed experimental characterization of the cobalt(III)−nitrene radical complexes, including the employment of several complementary spectroscopic techniques to explore further the (electronic) structure of these intriguing species.

CONCLUSIONS

The cobalt(II) porphyrin-catalyzed amination of aliphatic C−H bonds with organic azides has been shown to proceed

via a multistep radical-type mechanism. Coordination of an organic azide to the cobalt center followed by elimination of dinitrogen (**TS1**) produces an unusual "nitrene radical" intermediate (por)Co^{III}—$N^{\bullet}Y$ in which most of the unpaired spin density is localized at the "nitrene" nitrogen atom. Formation of these nitrene radical ligand complexes is an exothermic process, and hence, DFT calculations have predicted that nitrene radical ligand complexes should be detectable species in the absence of other reacting substrates. In good agreement, isotropic solution EPR signals with g values characteristic of ligand-based radicals that reveal hyperfine coupling with cobalt and a nitrogen nucleus were indeed detected experimentally in the spectra obtained from (por)Co complexes in the presence of an excess of organic azide. The "nitrene radical" intermediates are capable of abstracting a hydrogen atom from benzylic positions of the aromatic substrates (**TS2**) to form close-contact pairs of the thus-formed organic radicals $R'^{\bullet}$ and the cobalt(III)—amido species (por)Co^{III}—N*H*Y ($\{R'^{\bullet}\cdots$(por)Co^{III}—N*H*Y$\}$). These close-contact pairs easily collapse in a virtually barrierless fashion (**TS3**) to produce the desired N*H*YR′ amine products with regeneration of the Co(por) catalyst. Formation of the observed Y—NH_2 byproducts most likely involves β-hydrogen-atom abstraction from the benzylic radical $R'^{\bullet}$ in the close-contact radical—catalyst pair $\{R'^{\bullet}\cdots$(por)Co^{III}—N*H*Y$\}$ intermediates to form an olefin and (por)Co^{III}—NH_2Y. This olefin byproduct-forming process is also essentially barrierless and should compete with the desirable collapse of $\{R'^{\bullet}\cdots$(por)Co^{III}—N*H*Y$\}$ to form the amine products. Olefin formation via this radical-type β-hydrogen elimination has been confirmed experimentally. Elimination of dinitrogen from the azide adduct to form the "nitrene radical" intermediate (**TS1**) and subsequent benzylic hydrogen abstraction by this intermediate (**TS2**) are both kinetically important.

The herein-reported combined computational and experimental study has provided valuable information about the intimate reaction mechanism of these intriguing C—H amination reactions and shed new light on how to address selectivity issues in catalytic C—H amination reactions. This should aid future developments to expand the substrate scope and the design of new catalytic systems.

METHODS

Computational Methods. Geometry optimizations were carried out using the TURBOMOLE package[28] coupled with the PQS Baker optimizer[29] via the BOpt package[30] at the ri-DFT level using the BP86 functional and the resolution-of-identity (ri) method.[31] We used the SV(P) basis set[32] for the geometry optimizations of all stationary points. All minima (no imaginary frequencies) and transition states (one imaginary frequency) were characterized by numerically calculation of the Hessian matrix. Zero-point energy (ZPE) and gas-phase (GP) thermal corrections (entropy and enthalpy, 298 K, 1 bar) from these analyses were calculated. Improved energies were obtained with single-point calculations at the DFT/BP86 level using the TURBOMOLE def-TZVP basis set.[33] Estimated condensed-phase (1 L mol^{-1}) free energies and entropies were obtained from these data by neglecting the enthalpy RT term and subsequent correction for the condensed-phase (CP) reference volume [$S_{CP} = S_{GP} + R \ln(1/24.5)$] for all steps involving a change in the number of species, except for steps involving gaseous N_2.

EPR Spectroscopy. Samples of Co(3,5-Di^{t}Bu-ChenPhyrin)[34] and Co(TPP)[35] were prepared according to published procedures. They were dissolved in dry benzene-d_6, and an excess of the organic azide was added in a N_2-filled glovebox, after which the solution was transferred into a EPR tube. The samples were shaken for 10—30 min before measurements. Experimental X-band EPR spectra of these mixtures were recorded at room temperature on a Bruker EMX spectrometer located in Nijmegen. The spectra were simulated by iteration of the isotropic g values, hyperfine coupling constants, and line widths. We thank Prof. F. Neese for a copy of his EPR simulation program. Calculated EPR spectra were obtained at the DFT B3LYP/def2-TZVP level with the Turbomole-optimized geometries using ORCA[36].

ASSOCIATED CONTENT

Supporting Information. DFT-optimized geometries; tables containing ΔE, E_{ZPE}, ΔH, and ΔG values for all of the DFT-optimized geometries; and details of the EPR spectral simulations. This material is available free of charge via the Internet at http://pubs.acs.org.

AUTHOR INFORMATION

Corresponding Author
xpzhang@usf.edu; b.debruin@uva.nl

ACKNOWLEDGMENT

This work was financially supported by the European Research Council (Grant Agreement 202886 to B.d.B.), the University of Amsterdam (B.d.B.), the American Chemical Society (44286-AC1 to X.P.Z.), the National Science Foundation (CAREER Award CHE-0711024 to X.P.Z.), and the University of South Florida (X.P.Z.).

REFERENCES

(1) For recent reviews, see: (a) Godula, K.; Sames, D. *Science* **2006**, *312*, 67–72. (b) Labinger, J. A.; Bercaw, J. E. *Nature* **2002**, *417*, 507–514. (c) Shilov, A. E.; Shul'pin, G. B. *Chem. Rev.* **1997**, *97*, 2879–2932.

(2) For reviews, see: (a) Yeung, C. S.; Dong, V. M. *Chem. Rev.* **2011**, *111*, 1215–1292. (b) Chen, X.; Engle, K. M.; Wang, D.-H.; Yu, J.-Q. *Angew. Chem., Int. Ed.* **2009**, *48*, 5094–5115. (c) Le Bras, J.; Muzart, J. *Chem. Rev.* **2011**, *111*, 1170–1214.

(3) For reviews, see: (a) Davies, H. M. L.; Manning, J. R. *Nature* **2008**, *451*, 417–424. (b) Davies, H. M. L. *Angew. Chem., Int. Ed.* **2006**, *45*, 6422–6425.(c) Doyle, M. P. Synthetic Carbene and Nitrene Chemistry. In *Contemporary Reactive Intermediate Chemistry*; Moss, R. A., Platz, M. S., Jones, M., Jr., Eds.; Wiley: New York, 2004.

(4) For selected papers and reviews, see: (a) Sun, C.-L.; Li, B.-J.; Shi, Z.-J. *Chem. Rev.* **2011**, *111*, 1293–1314. (b) Bordeaux, M.; Galarneau, A.; Fajula, F.; Drone, J. *Angew. Chem., Int. Ed.* **2011**, *50*, 2075–2079. (c) Chen, H.; Schlecht, S.; Semple, T. C.; Hartwig, J. F. *Science* **2000**, *287*, 1995–1997. (d) Kniemeyer, O.; Musat, F.; Sievert, S. M.; Knittel, K.; Wilkes, H.; Blumenberg, M.; Michaelis, W.; Classen, A.; Bolm, C.; Joye, S. B.; Widdel, F. *Nature* **2007**, *449*, 898–901. (e) Barluenga, J.; González-Bobes, F.; González, J. M. *Angew. Chem., Int. Ed.* **2002**, *41*, 2556–2558.

(5) For reviews, see: (a) Driver, T. G. *Org. Biomol. Chem.* **2010**, *8*, 3831–3846. (b) Dick, A. R.; Sanford, M. S. *Tetrahedron* **2006**, *62*, 2439–2463. (c) Cenini, S.; Gallo, E.; Caselli, A.; Ragaini, F.; Fantauzzi, S.; Piangiolino, C. *Coord. Chem. Rev.* **2006**, *250*, 1234–1253. (d) Davies, H. M. L.; Long, M. S. *Angew. Chem., Int. Ed.* **2005**, *44*, 3518–3520. (e) Fantauzzi, S.; Caselli, A.; Gallo, E. *Dalton Trans.* **2009**, 5434–5443. (f) Collet, F.; Dodd, R. H.; Dauban, P. *Chem. Commun.* **2009**, 5061–5074. (g) Halfen, J. A. *Curr. Org. Chem.* **2005**, *9*, 657–669. (h) Collet, F.; Lescot, C.; Dauban, P. *Chem. Soc. Rev.* **2011**, *40*, 1926–1936. (i) Müller, P.; Fruit, C. *Chem. Rev.* **2003**, *103*, 2905–2919. (j) Lu, H.-J.; Zhang, X. P. *Chem. Soc. Rev.* **2011**, *40*, 1899–1909.

(6) For a review, see: (a) Dauban, P.; Dodd, R. H. In *Amino Group Chemistry: From Synthesis to the Life Sciences*; Ricci, A., Ed.; Wiley-VCH: Weinheim, Germany, 2008; pp 55—92. For selected recent examples of

intermolecular C−H amination with ArI═NTs, see:(b) Chang, J. W. W.; Chan, P. W. H. *Angew. Chem., Int. Ed.* **2008**, *47*, 1138–1140. (c) Li, Z.; Capretto, D. A.; Rahaman, R.; He, C. *Angew. Chem., Int. Ed.* **2007**, *46*, 5184–5186. (d) Liang, C.; Collet, F.; Robert-Peillard, F.; Müller, P.; Dodd, R. H.; Dauban, P. *J. Am. Chem. Soc.* **2008**, *130*, 343–350. (e) Chan, J.; Baucom, K. D.; Murry, J. A. *J. Am. Chem. Soc.* **2007**, *129*, 14106–14107. (f) Yang, J.; Weinberg, R.; Breslow, R. *Chem. Commun.* **2000**, 531–532.

(7) (a) Harden, J. D.; Ruppel, J. V.; Gao, G.-Y.; Zhang, X. P. *Chem. Commun.* **2007**, 4644–4646. (b) Albone, D. P.; Aujla, P. S.; Taylor, P. C. *J. Org. Chem.* **1998**, *63*, 9569–9571. (c) Albone, D. P.; Challenger, S.; Derrick, A. M.; Fillery, S. M.; Irwin, J. L.; Parsons, C. M.; Takada, H.; Taylor, P. C.; Wilson, D. J. *Org. Biomol. Chem.* **2005**, *3*, 107–111. (d) Fructos, M. R.; Trofimenko, S.; Díaz-Requejo, M. M.; Pérez, P. J. *J. Am. Chem. Soc.* **2006**, *128*, 11784–11791. For a theoretical mechanistic study, see:(e) Barman, D. N.; Liu, P.; Houk, K. N.; Nicholas, K. M. *Organometallics* **2010**, *29*, 3404–3412.

(8) (a) Lwowski, W.; Maricich, T. J. *J. Am. Chem. Soc.* **1965**, *87*, 3630–3637. (b) Lebel, H.; Huard, K.; Lectard, S. *J. Am. Chem. Soc.* **2005**, *127*, 14198–14199. (c) Clark, J. S.; Roche, C. *Chem. Commun.* **2005**, 5175–5177.

(9) (a) Lu, H.; Jiang, H.; Wojtas, L.; Zhang, X. P. *Angew. Chem., Int. Ed.* **2010**, *49*, 10192–10196. (b) Ruppel, J. V.; Kamble, R. M.; Zhang, X. P. *Org. Lett.* **2007**, *9*, 4889–4892. (c) Lu, H.; Tao, J.; Jones, J. E.; Wojtas, L.; Zhang, X. P. *Org. Lett.* **2010**, *12*, 1248–1251. (d) Lu, H.; Subbarayan, V.; Tao, J.; Zhang, X. P. *Organometallics* **2010**, *29*, 389–393. (e) Cenini, S.; Gallo, E.; Penoni, A.; Ragaini, F.; Tollari, S. *Chem. Commun.* **2000**, 2265–2266. (f) Ragaini, F.; Penoni, A.; Gallo, E.; Tollari, S.; Li Gotti, C.; Lapadula, M.; Mangioni, E.; Cenini, S. *Chem.—Eur. J.* **2003**, *9*, 249–259. (g) Caselli, A.; Gallo, E.; Fantauzzi, S.; Morlacchi, S.; Ragaini, F.; Cenini, S. *Eur. J. Inorg. Chem.* **2008**, 3009–3019. (h) Sun, K.; Sachwani, R.; Richert, K. J.; Driver, T. G. *Org. Lett.* **2009**, *11*, 3598–3601. (i) Badiei, Y. M.; Dinescu, A.; Dai, X.; Palomino, R. M.; Heinemann, F. W.; Cundari, T. R.; Warren, T. H. *Angew. Chem., Int. Ed.* **2008**, *47*, 9961–9964.

(10) For a review, see: (a) Espino, C. G.; Du Bois, J. In *Modern Rhodium-Catalyzed Organic Reactions*; Evans, P. A., Ed.; Wiley-VCH: Weinheim, Germany, 2005; pp 379−416. For selected papers, see:(b) Shen, M.; Leslie, B. E.; Driver, T. G. *Angew. Chem., Int. Ed.* **2008**, *47*, 5056–5059. (c) Stokes, B. J.; Dong, H.; Leslie, B. E.; Pumphrey, A. L.; Driver, T. G. *J. Am. Chem. Soc.* **2007**, *129*, 7500–7501. (d) Espino, C. G.; Wehn, P. M.; Chow, J.; Du Bois, J. *J. Am. Chem. Soc.* **2001**, *123*, 6935–6936. (e) Catino, A. J.; Nichols, J. M.; Forslund, R. E.; Doyle, M. P. *Org. Lett.* **2005**, *7*, 2787–2790.

(11) (a) Fantauzzi, S.; Gallo, E.; Caselli, A.; Ragaini, F.; Casati, N.; Macchic, P.; Cenini, S. *Chem. Commun.* **2009**, 3952–3954. (b) Liang, J.-L.; Yuan, S.-X.; Huang, J.-S.; Che, C.-M. *J. Org. Chem.* **2004**, *69*, 3610–3619. (c) Shou, W. G.; Li, J.; Guo, T.; Lin, Z.; Jia, G. *Organometallics* **2009**, *28*, 6847–6854.

(12) (a) Zhang, J.; Chan, P. W. H.; Che, C.-M. *Tetrahedron Lett.* **2005**, *46*, 5403–5408. For a review, see:(b) Abu-Omar, M. M. *Dalton Trans.* **2011**, *40*, 3435–3444.

(13) Liu, Y.; Che, C.-M. *Chem.—Eur. J.* **2010**, *16*, 10494–10501.

(14) (a) Chen, Y.; Ruppel, J. V.; Zhang, X. P. *J. Am. Chem. Soc.* **2007**, *129*, 12074–12075. (b) Zhu, S.; Perman, J. A.; Zhang, X. P. *Angew. Chem., Int. Ed.* **2008**, *47*, 8460–8463. (c) Zhu, S.-F.; Ruppel, J. V.; Lu, H.-J.; Wojtas, L.; Zhang, X. P. *J. Am. Chem. Soc.* **2008**, *130*, 5042–5043. (d) Zhu, S.-F.; Xu, X.; Perman, J. A.; Zhang, X. P. *J. Am. Chem. Soc.* **2010**, *132*, 12796–12799. For mechanistic investigations, see:(e) Dzik, W. I.; Xu, X.; Zhang, X. P.; Reek, J. N. H.; de Bruin, B. *J. Am. Chem. Soc.* **2010**, *132*, 10891–10902 and references therein. (f) Belof, J. L.; Cioce, C. R.; Xu, X.; Zhang, X. P.; Space, B.; Woodcock, H. L. *Organometallics* **2011**, *30*, 2739–2746. (g) Lu, H.; Dzik, W. I.; Xu, X.; Wojtas, L.; de Bruin, B.; Zhang, X. P. *J. Am. Chem. Soc.* **2011**, *133*, 8518–8521.

(15) (a) Gao, G.-Y.; Jones, J. E.; Vyas, R.; Harden, J. D.; Zhang, X. P. *J. Org. Chem.* **2006**, *71*, 6655–6658. (b) Ruppel, J. V.; Jones, J. E.; Huff, C. A.; Kamble, R. M.; Chen, Y.; Zhang, X. P. *Org. Lett.* **2008**, *10*, 1995–1998. (c) Jones, J. E.; Ruppel, J. V.; Gao, G.-Y.; Moore, T. M.; Zhang, X. P. *J. Org. Chem.* **2008**, *73*, 7260–7265. (d) Subbarayan, V.; Ruppel, J. V.; Zhu, S.; Perman, J. A.; Zhang, X. P. *Chem. Commun.* **2009**, 4266–4268.

(16) Hopmann, K. H.; Ghosh, A. *ACS Catal.* **2011**, *1*, 597–600.

(17) (a) Bigi, M. A.; Reed, S. A.; White, M. C. *Nat. Chem.* **2011**, *3*, 218–224. (b) King, E. R.; Hennessy, E. T.; Betley, T. A. *J. Am. Chem. Soc.* **2011**, *133*, 4917–4923.

(18) (a) Olivos Suarez, A. I.; Jiang, H.; Zhang, X. P.; de Bruin, B. *Dalton Trans.* **2011**, *40*, 5697–5705. (b) de Bruin, B.; Dzik, W. I.; Li, S.; Wayland, B. B. *Chem.—Eur. J.* **2009**, *15*, 4312–4320. (c) Li, S.; Peng, C.-H.; Fryd, M.; Wayland, B. B.; de Bruin, B. *J. Am. Chem. Soc.* **2008**, *130*, 13373–13381.

(19) (a) Chirik, P. J.; Wieghardt, K. *Science* **2010**, *327*, 794–795. (b) Dzik, W. I.; van der Vlugt, J. I.; Reek, J. N. H.; de Bruin, B. *Angew. Chem., Int. Ed.* **2011**, *50*, 3356–3358.(c) Dzik, W. I.; Zhang, X. P.; de Bruin, B. *Inorg. Chem.* [Online early access]. DOI: 10.1021/ic200043a. Published Online: April 26, 2011. (d) de Bruin, B.; Hetterscheid, D. G. H.; Koekkoek, A. J. J.; Grützmacher, H. *Prog. Inorg. Chem.* **2007**, *55*, 247–354. (e) de Bruin, B.; Hetterscheid, D. G. H. *Eur. J. Inorg. Chem.* **2007**, 211–230. (f) Boyer, J. L.; Rochford, J.; Tsai, M.-K.; Muckerman, J. T.; Fujita, E. *Coord. Chem. Rev.* **2010**, *254*, 309–330. (g) Ghosh, M.; Weyhermüller, T.; Wieghardt, K. *Dalton Trans.* **2010**, *39*, 1996–2007. (h) Kaim, W.; Schwederski, B. *Coord. Chem. Rev.* **2010**, *254*, 1580–1588.

(20) See Table S2 in the Supporting Information for a distribution of the Mulliken spin density values over the cobalt and nitrogen atoms.

(21) In a recent DFT-OLYP study employing *p*-NO_2-PhN_3 as the nitrene source, Hopmann and Ghosh reported very similar barriers for nitrene radical formation (+31 kcal mol^{-1}) and subsequent allylic hydrogen-atom abstraction from 2-methyl-1-butene (+27.4 kcal mol^{-1}). See ref 16.

(22) Complex **5a** was found to have a closed-shell singlet ground state at the B3LYP level of theory. The triplet species is ∼2 kcal mol^{-1} higher in energy. Attempts to locate an open-shell singlet (singlet biradical) electronic state in all cases led to transformation into a closed-shell species during the geometry optimizations.

(23) The related complex Rh(TMP)−OMe has an estimated Rh−O BDE of +46 kcal mol^{-1}. See: Sarkar, S.; Li, S.; Wayland, B. B. *J. Am. Chem. Soc.* **2010**, *131*, 13569–13571.

(24) Intermediate **9a** is 1.4 kcal mol^{-1} more stable than the transition state **TS7a** if ZPE is not taken into account. The transition state geometry optimization of the **TS7a** failed, since the calculations led to the more stable intermediate **7a**. We report here the energy of **TS7a** as a maximum on the potential energy surface obtained by constrained geometry optimization. For the whole reaction profile, see the Supporting Information.

(25) According to Mulliken population analysis at the BP86/def-TZVP level.

(26) The experimental spectrum of (TPP)Co($N^{\bullet}SO_2C_6H_4$*p*-NO_2) also revealed a sharp signal stemming from a small amount (∼1% of the total spectral intensity) of a free organic radical. The hyperfine couplings of this species with nitrogen (∼30 MHz) and possibly a deuterium (∼7 MHz) nucleus suggest that this is perhaps the free *p*-NO_2PhSO_2-$ND^{\bullet}$ radical. This species could be generated from (TPP)Co($N^{\bullet}SO_2C_6H_4$*p*-NO_2) upon reaction with trace amounts of D_2O in the solvent. For more details, see the Supporting Information.

(27) Isotropic A_{iso} values are averaged values of the anisotropic A_x, A_y, and A_z values. Since the computed anisotropic hyperfine couplings have both positive and negative values, small deviations can have a relatively large influence on the computed A_{iso} values. Nonetheless, the agreement between the experimental and computed values is decent.

(28) Ahlrichs, R. *TURBOMOLE*, version 5.8; Theoretical Chemistry Group, University of Karlsruhe: Karlsruhe, Germany, 2002.

(29) *PQS*, version 2.4; Parallel Quantum Solutions: Fayetteville, AR, 2001. The Baker optimizer (see:Baker, I. *J. Comput. Chem.* **1986**, *7*, 385–395) is available separately from Parallel Quantum Solutions upon request.

(30) Budzelaar, P. H. M. *J. Comput. Chem.* **2007**, *28*, 2226–2236.

(31) Sierka, M.; Hogekamp, A.; Ahlrichs, R. *J. Chem. Phys.* **2003**, *118*, 9136–9148.

(32) Schaefer, A.; Horn, H.; Ahlrichs, R. *J. Chem. Phys.* **1992**, *97*, 2571–2577.
(33) Eichkorn, K.; Weigend, F.; Treutler, O.; Ahlrichs, R. *Theor. Chem. Acc.* **1997**, *97*, 119–124.
(34) Chen, Y.; Fields, K. B.; Zhang, X. P. *J. Am. Chem. Soc.* **2004**, *126*, 14718–14719.
(35) Sugimoto, H.; Kuroda, K. *Macromolecules* **2008**, *41*, 312–317.
(36) Neese, F. *ORCA: An ab Initio Density Functional and Semiempirical Program Package*, version 2.8.0; University of Bonn: Bonn, Germany, 2009.